MATHEMATICAL MODELING OF THREE-DIMENSIONAL DIE FLOWS OF VISCOPLASTIC FLUIDS WITH WALL SLIP

Adeniyi Lawal, Sudhir Railkar and Dilhan M. Kalyon
Highly Filled Materials Institute
Stevens Institute of Technology
Castle Point, Hoboken, NJ 07030

Abstract

The mathematical modeling of the continuous processing of filled polymers, and concentrated suspensions in screw extruders and dies of complex shapes is undertaken. The simulation of the flow of such filled systems in complex geometries is rendered complicated by the occurrence of wall slip at fluid/solid boundaries. The incorporation of wall slip in the analysis of three-dimensional flows including flows through dies, single/twin-screw extruders and other processing geometries is currently lacking. Here we present an analysis of three-dimensional flows with wall slip, and demonstrate the procedure using the flow of a Herschel-Bulkley fluid in a tapered die.

Introduction

Single/Twin-screw extruders in combination with dies of complex shapes are used in the extrusion of filled polymers and concentrated suspensions. The processing and simulation of the continuous processing of such filled systems are affected by their viscoplasticity and the occurrence of apparent wall slip. Various simplified mathematical models are available for describing the flow and deformation history experienced by these materials in complex geometries, but the flows are usually three-dimensional and at present, no method has been reported in the literature for the rigorous incorporation of slip at the wall for these types of flows. In what follows, we present such a modeling procedure that is based on the Finite Element Method, and we demonstrate the procedure using a Herschel-Bulkley fluid that exhibits a wall slip coefficient that is dependent on the second invariant of the viscous stress tensor.

Analysis

Flow Equations

The flow in the extruder/die is governed by the equations of conservation of mass and momentum, which are three-dimensional and fully-elliptic. The flow is steady and for this demonstration analysis it is assumed to be isothermal. The inertia effect is negligible because of the highly viscous nature of materials of interest i.e., polymeric melts, suspensions, blends, etc., and the creeping nature of the resulting flow. The following dimensionless variables are introduced:

$$x = R_s x^*, y = R_s y^*, z = R_s z^*, \underline{u} = R_s \omega \underline{u}^* \quad (1a)$$

$$\eta = m_o \omega^{n-1} \eta^*, Q = R_s^3 \omega Q^*, p = m_o \omega^n p^* \quad (1b)$$

where R_s is the screw radius of the twin screw extruder preceding the die, ω is the screw rotational speed, m_o and n are parameters of the generalized Newtonian fluid with the shear viscosity material function of η, $\underline{u}$ is the velocity vector, p is pressure and Q is the volumetric flow rate. The applicable equations of conservation of mass and momentum are then:

$$\nabla \cdot \underline{u} = 0 \quad (2)$$

$$\nabla \cdot \underline{\underline{T}} = \underline{0} \quad (3)$$

where $\underline{\underline{T}}$ is the total stress tensor. The penalty/ Galerkin Finite Element Method is employed. In this method, the continuity equation is considered as a constraint on the equations of conservation of momentum and pressure p is approximated by using a large positive number λ_p (penalty parameter):

$$p = -\lambda_p \eta \left(\frac{\partial u_x}{\partial x} + \frac{\partial u_y}{\partial y} + \frac{\partial u_z}{\partial z} \right) \quad (4)$$

A penalty parameter of 10^6 generally produces satisfactory results. When Eq. (4) is substituted into Eq. (3) with a generalized Newtonian fluid with shear viscosity η the equations of conservation of momentum become:

$$-\frac{\partial}{\partial x}\left[\lambda_p \eta \left(\frac{\partial u_x}{\partial x} + \frac{\partial u_y}{\partial y} + \frac{\partial u_z}{\partial z} \right) \right] = \frac{\partial}{\partial x}\left(2\eta \frac{\partial u_x}{\partial x} \right)$$
$$+ \frac{\partial}{\partial y}\left(\eta \left(\frac{\partial u_x}{\partial y} + \frac{\partial u_y}{\partial x} \right) \right) + \frac{\partial}{\partial z}\left(\eta \left(\frac{\partial u_z}{\partial x} + \frac{\partial u_x}{\partial z} \right) \right) \quad (5a)$$

$$-\frac{\partial}{\partial y}\left[\lambda_p \eta\left(\frac{\partial u_x}{\partial x}+\frac{\partial u_y}{\partial y}+\frac{\partial u_z}{\partial z}\right)\right]=\frac{\partial}{\partial x}\left(\eta\left(\frac{\partial u_x}{\partial y}+\frac{\partial u_y}{\partial x}\right)\right)$$
$$+\frac{\partial}{\partial y}\left(2\eta\frac{\partial u_y}{\partial y}\right)+\frac{\partial}{\partial z}\left(\eta\left(\frac{\partial u_y}{\partial z}+\frac{\partial u_z}{\partial y}\right)\right) \qquad (5b)$$

$$-\frac{\partial}{\partial z}\left[\lambda_p \eta\left(\frac{\partial u_x}{\partial x}+\frac{\partial u_y}{\partial y}+\frac{\partial u_z}{\partial z}\right)\right]=\frac{\partial}{\partial x}\left(\eta\left(\frac{\partial u_z}{\partial x}+\frac{\partial u_x}{\partial z}\right)\right)$$
$$+\frac{\partial}{\partial y}\left(\eta\left(\frac{\partial u_y}{\partial z}+\frac{\partial u_z}{\partial y}\right)\right)+\frac{\partial}{\partial z}\left(2\eta\frac{\partial u_z}{\partial z}\right) \qquad (5c)$$

Boundary Conditions and Implementation of Wall Slip

Applying Bubnov-Galerkin's method to Eq. 3 leads to the following dimensionless residual equations:

$$\int_V \nabla\phi^i \cdot \underline{\underline{T}}dV-\int_D \phi^i(\underline{n}\cdot\underline{\underline{T}})dD=\underline{0} \qquad (6)$$

where ϕ^i is the weighting function and $\underline{\underline{T}}$ is the total stress tensor. On the fluid/fluid interface, i.e., at the entrance and exit planes, since the velocity distribution is usually not known, the boundary term in Eq. 6 is expressed in terms of the traction boundary conditions and takes the form:

$$\int_{Fluid/Fluid}\phi^i(\underline{n}\cdot\underline{\underline{T}})dD=-\int_{Fluid/Fluid}\phi^i(t_x\underline{i}+t_y\underline{j}+t_z\underline{k})dD \qquad (7)$$

where

$$t_x=2\eta\frac{\partial u_x}{\partial x}n_x+\eta\left(\frac{\partial u_x}{\partial y}+\frac{\partial u_y}{\partial x}\right)n_y+$$
$$\eta\left(\frac{\partial u_z}{\partial x}+\frac{\partial u_x}{\partial z}\right)n_z-pn_x \qquad (8a)$$

$$t_y=\eta\left(\frac{\partial u_x}{\partial y}+\frac{\partial u_y}{\partial x}\right)n_x+2\eta\frac{\partial u_y}{\partial y}n_y+$$
$$\eta\left(\frac{\partial u_y}{\partial z}+\frac{\partial u_z}{\partial y}\right)n_z-pn_y \qquad (8b)$$

$$t_z=\eta\left(\frac{\partial u_z}{\partial x}+\frac{\partial u_x}{\partial z}\right)n_x+\eta\left(\frac{\partial u_y}{\partial z}+\frac{\partial u_z}{\partial y}\right)n_y+$$
$$2\eta\frac{\partial u_z}{\partial z}n_z-pn_z \qquad (8c)$$

and n_x, n_y, and n_z are the components of the unit outward normal vector, $\underline{n}$ at the interface. On the fluid/solid boundaries, the traction $\underline{n}\cdot\underline{\underline{T}}$ can be decomposed into the tangential and normal components to obtain:

$$\int_{Fluid/Solid}\phi^i(\underline{n}\cdot\underline{\underline{T}})dD=$$
$$\int_{Fluid/Solid}\phi^i\left[(\underline{n}\underline{t}_1:\underline{\underline{T}})\underline{t}_1+(\underline{n}\underline{t}_2:\underline{\underline{T}})\underline{t}_2+(\underline{n}\underline{n}:\underline{\underline{T}})\underline{n}\right]dD \qquad (9)$$

where $\underline{t}_1$, $\underline{t}_2$, and $\underline{n}$ are the unit tangents and outward unit normal vectors to the fluid/solid boundary respectively. Equations 2 and 3 are required to be satisfied on the fluid/solid boundaries. The tangential components can be related to the slip velocity through the Navier's wall slip boundary condition which in its general form (Silliman and Scriven (1)), is given by:

$$\underline{\underline{I}}_{II}\cdot(\underline{u}-\underline{u}_{solid})=\beta\underline{\underline{I}}_{II}\cdot(\underline{n}\cdot\underline{\underline{T}}) \qquad (10)$$

where β is the slip coefficient, and $\underline{\underline{I}}_{II}$ is the geometric tensor for a surface. If the slip coefficient is dependent on the second invariant of the stress tensor, the tangential components can be expressed as:

$$\underline{t}_1\underline{n}:\underline{\underline{T}}=\frac{\underline{t}_1\cdot(\underline{u}-\underline{u}_{solid})}{\alpha\left[(\underline{\underline{\tau}}:\underline{\underline{\tau}})/2\right]^{(s_b-1)/2}} \qquad (11a)$$

$$\underline{t}_2\underline{n}:\underline{\underline{T}}=\frac{\underline{t}_2\cdot(\underline{u}-\underline{u}_{solid})}{\alpha\left[(\underline{\underline{\tau}}:\underline{\underline{\tau}})/2\right]^{(s_b-1)/2}} \qquad (11b)$$

where the parameters α and s_b are obtained from the rheological characterization of the material.The normal component presents a difficulty as it is not recoverable from the kinematic boundary condition which gives only the normal velocity. The numerical difficulty is resolved by transforming the essential condition of normal velocity into a natural condition through:

$$\underline{n}\underline{n}:\underline{\underline{T}}=\frac{\underline{n}\cdot(\underline{u}-\underline{u}_{solid})}{\lambda_s} \qquad (12)$$

where a new penalty parameter λ_s, has been introduced. As $\lambda_s \to 0$, Eq. (12) becomes equivalent to the kinematic condition, since the normal component of the traction must be finite at the boundary. At the die walls, the components of $\underline{u}_{solid}$ are all zero. On the other hand, for rotating screw elements, $\underline{u}_{solid}$ is of the form:

$$\underline{u}=\omega r\underline{e}_\theta \qquad (13)$$

where r is the radial position of any point on the screw with respect to the center of that rotating screw and $\underline{e}_\theta$ is the unit vector in the θ direction.

Constitutive Equation

The fluid is assumed to be a purely viscous fluid that can be characterized by the generalized Newtonian fluid. The following dimensionless variables are introduced.

$$|\dot{\gamma}| = \omega|\dot{\gamma}|^{*} \;, \tau_y = m_0\omega^n\tau_y^{*} \;, n_b = \frac{n_b^{*}}{\omega} \quad (14)$$

The dependence of the shear viscosity material function η, on the deformation rate is assumed to follow the generalized Newtonian fluid behavior i.e., modified Herschel-Bulkley equation following Papanastasiou (2) for viscoplastic fluids or its simplification the Ostwald-de Waele or Power Law fluid with $\tau_y = 0$:

$$\eta = \left[m_0 (|\dot{\gamma}|)^{n-1} + \frac{\tau_y (1-\exp(-n_b|\dot{\gamma}|))}{|\dot{\gamma}|} \right] \exp(-c'(T-T_0)) \quad (15)$$

where n is the power law index, τ_y is the yield stress, n_b is the stress growth exponent, c' is the activation energy and T_0 is the reference temperature at which m_0 is determined. The magnitude of the rate of deformation tensor $|\dot{\gamma}|$ is :

$$|\dot{\gamma}|^2 = 2u_{x,x}^2 + 2u_{y,y}^2 + 2u_{z,z}^2 + (u_{x,y}+u_{y,x})^2 + (u_{x,z}+u_{z,x})^2 + (u_{y,z}+u_{z,y})^2 \quad (16)$$

where the comma indicates differentiation. Simplifications of the modified Herschel-Bulkley equation are the Ostwald-de-Waele power law fluid ($\tau_y = 0$), the Newtonian fluid ($n = 1, \tau_y = 0$), the modified Bingham plastic (n = 1), and the Bingham plastic fluid above the yield point ($n = 1$, $n_b = \infty$). Our simulation approach will be demonstrated here with a viscoplastic fluid obeying the Herschel-Bulkley equation.

Numerical Solution

For FEM solution of the momentum equations, the domain is discretized by the trilinear brick elements in x, y and z, and trial functions:

$$u_x = \sum_{j=1}^{Nod} u_x^j \phi^j(x,y,z) \quad (17a)$$

$$u_y = \sum_{j=1}^{Nod} u_y^j \phi^j(x,y,z) \quad (17b)$$

$$u_z = \sum_{j=1}^{Nod} u_z^j \phi^j(x,y,z) \quad (17c)$$

$$u_x^j, u_y^j, u_z^j, \phi^j \in V^e \quad (17d)$$

where V^e is an element domain, Nod is the number of nodes per element, and ϕ^j is the trial function. The weak form of the weighted residual equation is given below:

$$\int_{V^e} \left\{ \begin{array}{l} 2\eta \frac{\partial\phi^i}{\partial x}\frac{\partial u_x}{\partial x} + \eta\frac{\partial\phi^i}{\partial y}\left(\frac{\partial u_x}{\partial y}+\frac{\partial u_y}{\partial x}\right) + \\ \eta\frac{\partial\phi^i}{\partial z}\left(\frac{\partial u_z}{\partial x}+\frac{\partial u_x}{\partial z}\right) \end{array} \right\} dxdydz + \lambda_p \int_{V^e} \eta\frac{\partial\phi^i}{\partial x}\left(\frac{\partial u_x}{\partial x}+\frac{\partial u_y}{\partial y}+\frac{\partial u_z}{\partial z}\right) dxdydz$$
$$- \int_{Fluid/Fluid} \phi^i t_x dD + \int_{Fluid/Solid} \frac{(\underline{i}\cdot\underline{t}_1)\underline{t}_1\cdot(\underline{u}-\underline{u}_{solid})\phi^i}{\alpha\left[(\underline{\underline{\tau}}:\underline{\underline{\tau}})/2\right]^{(s_b-1)/2}} dD + \int_{Fluid/Solid} \frac{(\underline{i}\cdot\underline{n})\underline{n}\cdot(\underline{u}-\underline{u}_{solid})\phi^i}{\lambda_s} dD +$$
$$\int_{Fluid/Solid} \frac{(\underline{i}\cdot\underline{t}_2)\underline{t}_2\cdot(\underline{u}-\underline{u}_{solid})\phi^i}{\alpha\left[(\underline{\underline{\tau}}:\underline{\underline{\tau}})/2\right]^{(s_b-1)/2}} dD = 0 \quad (18a)$$

$$\int_{V^e} \left\{ \begin{array}{l} 2\eta \frac{\partial\phi^i}{\partial y}\frac{\partial u_z}{\partial y} + \eta\frac{\partial\phi^i}{\partial x}\left(\frac{\partial u_z}{\partial y}+\frac{\partial u_x}{\partial x}\right) \\ + \eta\frac{\partial\phi^i}{\partial z}\left(\frac{\partial u_y}{\partial z}+\frac{\partial u_z}{\partial y}\right) \end{array} \right\} dxdydz + \lambda_p \int_{V^e} \eta\frac{\partial\phi^i}{\partial y}\left(\frac{\partial u_x}{\partial x}+\frac{\partial u_y}{\partial y}+\frac{\partial u_z}{\partial z}\right) dxdydz$$
$$- \int_{Fluid/Fluid} \phi^i t_y dD + \int_{Fluid/Solid} \frac{(\underline{j}\cdot\underline{t}_1)\underline{t}_1\cdot(\underline{u}-\underline{u}_{solid})\phi^i}{\alpha\left[(\underline{\underline{\tau}}:\underline{\underline{\tau}})/2\right]^{(s_b-1)/2}} dD + \int_{Fluid/Solid} \frac{(\underline{j}\cdot\underline{n})\underline{n}\cdot(\underline{u}-\underline{u}_{solid})\phi^i}{\lambda_s} dD +$$
$$\int_{Fluid/Solid} \frac{(\underline{j}\cdot\underline{t}_2)\underline{t}_2\cdot(\underline{u}-\underline{u}_{solid})\phi^i}{\alpha\left[(\underline{\underline{\tau}}:\underline{\underline{\tau}})/2\right]^{(s_b-1)/2}} dD = 0 \quad (18b)$$

$$
\begin{aligned}
&\int_{V^e} \left\{ \begin{array}{l} 2\eta \dfrac{\partial \phi^i}{\partial z}\dfrac{\partial u_z}{\partial z} + \eta \dfrac{\partial \phi^i}{\partial x}\left(\dfrac{\partial u_z}{\partial x} + \dfrac{\partial u_x}{\partial z}\right) \\ + \eta \dfrac{\partial \phi^i}{\partial y}\left(\dfrac{\partial u_y}{\partial z} + \dfrac{\partial u_z}{\partial y}\right) \end{array} \right\} dxdydz \\
&+ \lambda_p \int_{V^e} \eta \frac{\partial \phi^i}{\partial z}\left(\frac{\partial u_x}{\partial x} + \frac{\partial u_y}{\partial y} + \frac{\partial u_z}{\partial z}\right) dxdydz \\
&- \int_{Fluid/Fluid} \phi^i t_z dD + \int_{Fluid/Solid} \frac{(\underline{k} \cdot \underline{t}_1)\underline{t}_1 \cdot (\underline{u} - \underline{u}_{solid})\phi^i}{\alpha\left[(\underline{\underline{\tau}} : \underline{\underline{\tau}})/2\right]^{(s_b - 1)/2}} dD \\
&+ \int_{Fluid/Solid} \frac{(\underline{k} \cdot \underline{n})\underline{n} \cdot (\underline{u} - \underline{u}_{solid})\phi^i}{\lambda_s} dD + \\
&\int_{Fluid/Solid} \frac{(\underline{k} \cdot \underline{t}_2)\underline{t}_2 \cdot (\underline{u} - \underline{u}_{solid})\phi^i}{\alpha\left[(\underline{\underline{\tau}} : \underline{\underline{\tau}})/2\right]^{(s_b - 1)/2}} dD = 0 \qquad (18c)
\end{aligned}
$$

The components of the unit tangent and unit normal vectors needed in the evaluation of the boundary terms in Eqs. (18a-c) are obtainable from the components of the Jacobian matrix for the transformation from global coordinates x, y, and z to the natural coordinates. Equations (17a-c) are substituted into Eqs. (18a-c), and all numerical integrations are performed in the natural coordinates using a 2 x 2 x 2 Gauss quadrature except for the penalty terms which are evaluated using reduced integration (i.e., 1 x 1 x 1 Gauss quadrature). The FEM mesh used here has 9952 elements and 11375 nodes. The solution involves a degree of freedom of 34125 and a stiffness matrix with over 56 million entries. The simulations were performed on a Silicon Graphics Power Challenge computer with six parallel processors

Results and Discussion

The wall slip behavior of a concentrated suspension is demonstrated in Fig.1 where upon deformation of the suspension in a rotational viscometer, discontinuities appear on the straight line marker at suspension/wall interfaces. The material used for the demonstration of the modeling procedure was characterized for its wall slip behavior using the Instron Capillary Rheometer with a series of capillaries with different diameters and length/diameter ratios. The wall slip velocity versus the wall shear stress behavior of the material is shown in Fig. 2, indicating a wall slip coefficient that is dependent on the second invariant of the viscous stress tensor. The material parameters of this Herschel-Bulkley fluid are m=28,000Pa.s^n, n=.49, τ_y = 60,000Pa, α^*=5.53x10^{-4} and s_b=1.235, and its flow was simulated in the tapered die shown in Fig. 3. Figure 4 shows the cross-sectional axial velocity distributions at a selected axial location of the die, with and without wall slip. In Fig. 4b., a finite no-zero u_z value occurs at the wall on account of wall slip. For the conditions simulated, at a pressure drop of 1.55 MPa, the flow rate when wall slip is taken into consideration is 114 kg/h in comparison with 90 kg/h for the no slip condition, a difference of about 26% which is quite significant for design purposes.

References

1. Silliman, W. T. and L. E. Scriven, *J. Comput. Phys*., 34, 287 (1980).
2. Papanastasiou, T.C., *J. Rheol*., 31, 385 (1987).

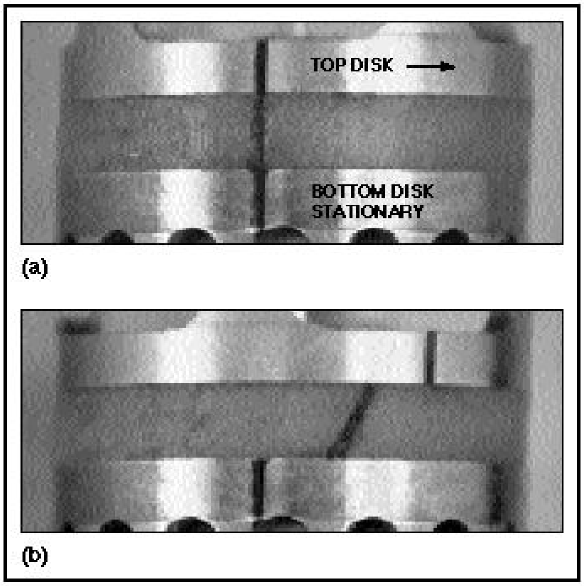

Figure 1. Demonstration of wall slip behavior of a concentrated suspension.

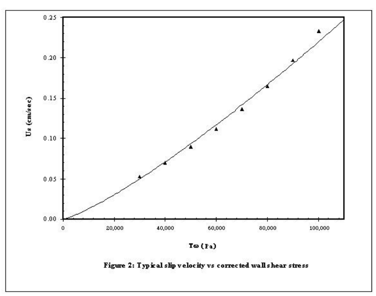

Figure 2. Slip velocity vs. shear stress

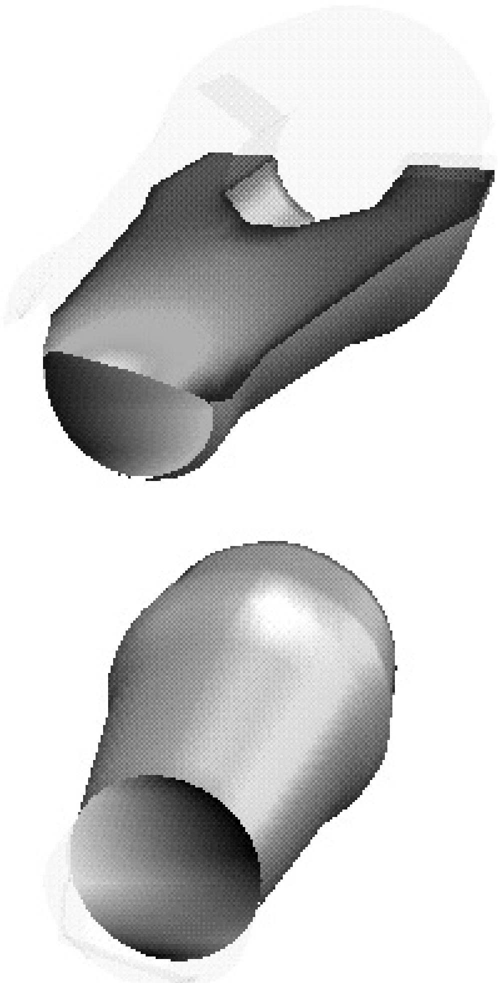

Figure 3. Geometry of the die

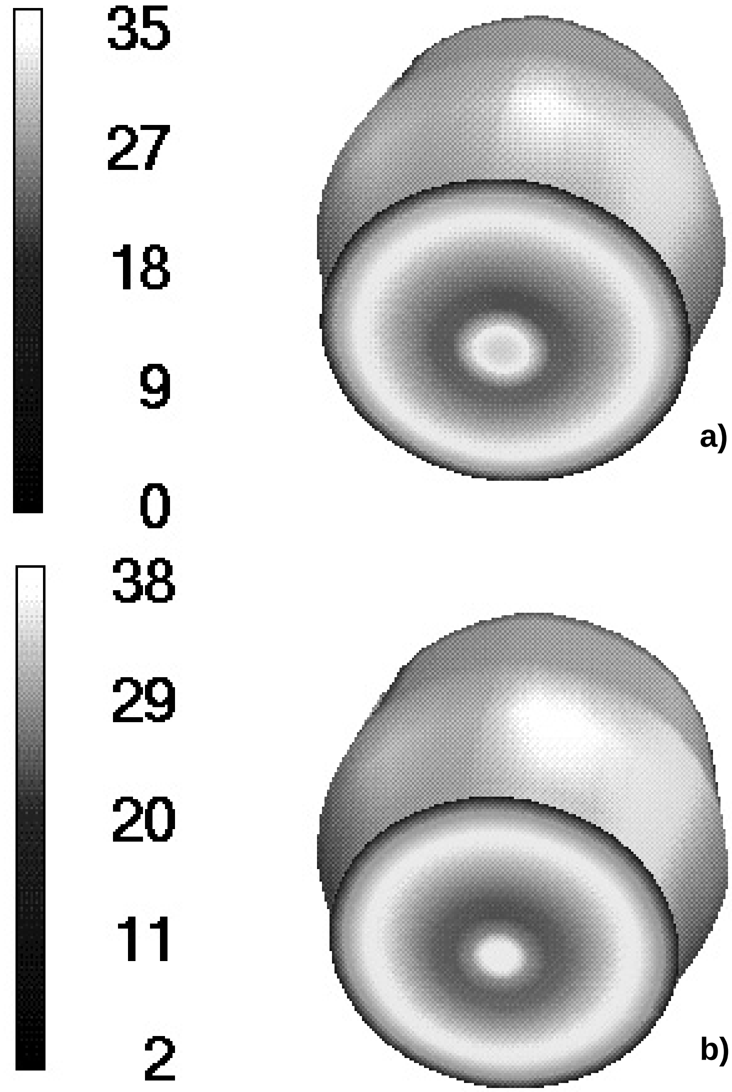

Figure 4: Z-velocity distribution for a viscoplastic fluid at a pressure drop of 1.55 Mpa a) noslip b) slip